Title
TGF-β Activity Is Prognostic in Medulloblastoma

Journal
Brain Pathology, 23(2)

ISSN
1015-6305

Authors
Aref, Donya
Moffatt, Connor J
Agnihotri, Sameer
et al.

Publication Date
2013-03-01

DOI
10.1111/j.1750-3639.2012.00631.x

Peer reviewed

Brain Pathology ISSN 1015-6305

RESEARCH ARTICLE

Canonical TGF-β Pathway Activity Is a Predictor of SHH-Driven Medulloblastoma Survival and Delineates Putative Precursors in Cerebellar Development

Donya Aref[1,2,3]; Connor J. Moffatt[2,3]; Sameer Agnihotri[2]; Vijay Ramaswamy[2]; Adrian M. Dubuc[2]; Paul A. Northcott[2]; Michael D. Taylor[2]; Arie Perry[4]; James M. Olson[5]; Charles G. Eberhart[6] and Sidney E. Croul[1,2,3]

[1] Department of Laboratory Medicine and Pathobiology, Faculty of Medicine, University of Toronto, Toronto, ON, Canada.
[2] Arthur and Sonia Labatt Brain Tumor Research Centre, Hospital for Sick Children, University of Toronto, Toronto, ON, Canada.
[3] Department of Pathology, University Health Network, University of Toronto, Toronto, ON, Canada.
[4] Division of Neuropathology, University of California in San Francisco, San Francisco, CA.
[5] Department of Laboratory Medicine, Fred Hutchinson Cancer Research Center, University of Washington/Children's Hospital, Seattle, WA.
[6] Department of Pathology, Johns Hopkins University, Baltimore, MD.

Keywords
medulloblastoma, prognosis, Smad3, TGF beta.

Corresponding author:
Sidney Croul, MD, FRCPC, Lab Med and Pathobiology, University of Toronto, Toronto, ON, Canada M5G 2C4 (E-mail: *sidney.croul@uhn.on.ca*)

Received 12 June 2012
Accepted 30 August 2012
Published Online Article Accepted 12 September 2012

doi:10.1111/j.1750-3639.2012.00631.x

Abstract

Medulloblastoma (MB) is the most common malignant brain tumor of childhood. Very little is known about aggressive forms of this disease, such as metastatic or recurrent MBs. In order to identify pathways involved in aggressive MB pathophysiology, we performed unbiased, whole genome microarrays on MB tumors at both the human and murine levels. Primary human MBs were compared, transcriptomically, to their patient-matched recurrent or metastatic tumors. Expression profiling was also performed on murine tumors from two spontaneously developing MB mouse models (Ptch+/– and Smo/Smo) that present with differing clinical severities. At both the human and murine levels we identified transforming growth factor-beta (TGF-β) as a potential contributor to MB progression/metastasis. Smad3, a major downstream component of the TGF-β pathway, was also evaluated using immunohistochemistry in malignant human tissues and was shown to correlate with MB metastasis and survival. Similarly, Smad3 expression during development identified a subset of cerebellar neuronal precursors as putative cells of origin for the Smad3-positive MBs. To our knowledge, this is the first study that links TGF-β to MB pathogenesis. Our research suggests that canonical activation of this pathway leads to better prognosis for patients.

INTRODUCTION

Medulloblastoma (MB) is the most common malignant brain tumor of childhood. It arises in the cerebellum and has a tendency to metastasize to the leptomeningeal covering of the central (CNS) and peripheral nervous system (PNS). This tumor is classified as a primitive neuroectodermal tumor and thought to arise from transformed cells during cerebellar development (16, 22, 43). Although, with current treatment regimens, survival of average risk patients has significantly improved, most with progressive and/or metastatic disease still remain incurable (5, 8, 53). Little is known about the underlying biology that mediates enhanced malignancy, marked by increased growth and decreased responsiveness to therapy, characteristic of recurrent or metastatic MB (8, 11, 46, 53). In addition, because of the aggressive nature of therapy, many survivors suffer from long-term treatment associated sequelae, such as neurocognitive deficits, endocrine disorders and formation of secondary tumors (4, 40). Therefore, there is a need to better understand the pathophysiology of this tumor and develop better prognosticators to risk stratify patients and spare as many as possible from highly damaging aggressive treatment.

Traditionally, one of the major criteria used for risk stratification of patients has been based on the histological classification of their tumors (4, 11, 31, 40). However, this has had various associated problems, including inconsistencies in interpretation between different pathologists, the difficulty of defining subtle features and most importantly, an inability to fully and consistently identify high- vs. low-risk patients (4). With the advent of high throughput techniques to profile the protein expression and genetic landscape of tumors, a different classification system for MB has been developed (5, 10, 30, 31, 36, 48). Through this type of analysis at the RNA and DNA level of a large cohort of samples derived from primary tumors, various groups have determined that like many other cancers, MB is not a homogenous disease but is composed of at least four broad subtypes that display differing genetic aberrations, transcriptomic profiles and pathophysiological behaviors (5, 10, 30, 31, 36, 48). In spite of these advances, little remains known about mediators of aggressive MB behavior.

To identify pathways, which are involved in the progression of MB from a localized primary tumor to a more aggressive and potentially metastatic cancer, we performed global gene expression microarrays, comparing human primary MBs with patient-matched recurrences/metastases. This data was supplemented with a similar comparison between indolent and aggressive tumors derived from two mouse models that spontaneously develop MB: Ptch+/– and Smo/Smo (refs).

With this approach, we have identified the transforming growth factor (TGF)-β signaling pathway as a potential contributor to MB pathogenesis and aggressive behavior. Validation of our microarray data, via immunohistochemistry, confirmed our array results. To our knowledge, this is one of the first studies that directly links the TGF-β pathway to MB pathogenesis.

MATERIALS AND METHODS

MB samples for RNA expression profiling

Review of University Health Network (UHN) archival materials from 1962 to 2010 identified 10 adult patients for whom formalin-fixed paraffin-embedded (FFPE) samples of both primary and subsequent recurrent and/or metastatic MBs were available for study. These cases were supplemented with material from Washington University in St Louis (A. Perry) representing an additional 12 adult and pediatric patients fulfilling the same criteria. Murine fresh frozen primary MBs from Ptch+/– knockout mice were provided by M.D. Taylor, Hospital for Sick Children, Toronto. Fresh frozen cerebella from Smo/Smo mice, sacrificed because of tumor burden, were provided by J.M. Olson, University of Washington, Fred Hutchinson Cancer Center. All human and murine samples were obtained and accessed in accordance with institutional research ethics guidelines.

Smad3 mRNA expression levels in primary MBs

Access to two previously described gene expression profiling databases of primary MBs (5, 36) was granted by MD Taylor, Hospital for Sick Children, Toronto. Separation of high- vs. low-Smad3 mRNA expressers was defined by samples with expression greater/less than the median expression.

Molecular subtyping of human samples by NanoString

100–200 ng of RNA from the eight human adult samples profiled in the microarray experiment, was used to identify the molecular subgroup of the tumors via NanoString nCounter Technology as described previously (37).

RNA extraction from human samples

Ten-micron thick scrolls were cut from human FFPE MB samples that consisted of >80% tumor and deparaffinized by using successive 30-minute incubations with xylene, 90% ethanol, 70% ethanol and, finally, water. RNA was extracted using the Roche High Pure RNA Paraffin Kit (Roche Applied Science, Penzberg, Germany) according to manufacturer's protocol. RNA quantity and purity was assessed by spectrophotometry (NanoDrop 1000; NanoDrop Technologies Inc., Wilmington, DE, USA) and only samples that gave sufficient (>90 ng/μL) and pure RNA (260/280 ≥ 1.7) were used for further processing.

RNA extraction from murine samples

Sections were cut from the fresh frozen cerebella of Smo/Smo mice and stained with Hematoxylin and Eosin (HE) staining. Tumor location was identified and areas that represented >80% tumor were excised for RNA extractions. RNA was isolated from all murine samples using the Qiagen Rneasy Mini kit (Qiagen, Hilden, Germany) according to manufacturer's protocol. RNA quantity and quality was evaluated by spectrophotometry (NanoDrop 1000; NanoDrop Technologies Inc.) and microfluidics-based electrophoresis (Agilent 2100 Bioanalyzer; Agilent Technologies, Santa Clara, CA, USA). All murine samples used for the microarray study had an RNA Integrity Number (RIN) ≥8.5 and a 260/280 ≥ 1.8.

Human microarray experiments

200 ng from each of the RNA samples were labeled and amplified following Illumina Whole Genome Gene Expression-cDNA-mediated Annealing, Selection, extension and Ligation (DASL) assay kit (Illumina Inc., San Diego, CA, USA) for partially degraded and FFPE-derived samples. The labeled samples were then hybridized onto a Human Ref-8 V3 BeadChip (Illumina Inc.). The BeadChip was incubated at 58°C, for 18 h to allow hybridization. The BeadChip was washed as per Illumina protocol and scanned on the iScan (Illumina). The data files were quantified in GenomeStudio Version 2010.2 (Illumina).

Murine microarray experiments

200 ng of RNA from Ptch+/– ($n = 3$) and Smo/Smo ($n = 3$) tumors were labeled using Illumina TotalPrep-96 RNA amplification kit (Ambion, Life Technologies, Carlsbad, CA, USA) as per amplification protocol. 1.5 ng of cRNA generated from these six samples was used to hybridize onto a Mouse WG-6 V2 BeadChip platform. The BeadChip was incubated at 58°C, for 17.5 h to allow hybridization. The BeadChip was washed and stained as per Illumina protocol and scanned on the iScan (Illumina). The data files were quantified in GenomeStudio Version 2010.2 (Illumina).

Microarray data analysis

Invariant normalization was performed on $\log_2$-transformed data using the D-chip (33) program. Using the t-mev program (44, 45) the gene list was first filtered to remove genes whose expression did not change between samples up to the 20th percentile. Significant genes were then identified using *t*-tests with a standard Bonferroni correction ($P = 0.05$) in t-mev. Genes with an absolute fold change value of less than 1.5 were excluded from our final list. Bioinformatics analysis was performed using the Ingenuity Pathway Analysis (IPA) program. A dataset containing gene identifiers and corresponding expression values was uploaded into the application. Each identifier was mapped to its corresponding object in the Ingenuity Knowledge Base. An absolute fold change value cut off of 1.5 was set to identify molecules whose expression

was significantly differentially regulated. These molecules, called network eligible molecules, were overlaid onto a global molecular network developed from information contained in the Ingenuity Knowledge Base. Networks of network eligible molecules were then algorithmically generated based on their connectivity.

Tissues for immunohistochemistry

A tissue microarray (TMA) was constructed from the total number of UHN and Washington University in St Louis specimens. The UHN archive from 1962 to 2010 yielded a total of 49 MB samples from 28 adult and three pediatric patients. Washington University in St Louis samples provided an additional 27 samples from eight pediatric and four adult patients. An additional TMA of human MBs for analysis was provided by C. Eberhardt, Johns Hopkins Hospital, Baltimore, MD, USA. This TMA was constructed using primary samples from 55 pediatric and adult patients (11 adults, 40 pediatric, 4 unknown age). Survival data was known for 49/55 patients. All 55 samples were histologically and molecularly subtyped. 36/55 samples exhibited a classic histology; 12/55 exhibited desmoplastic histology and 7/55 exhibited large cell anaplastic histology. The samples were molecularly subtyped by immunohistochemistry. 1/55 tumors was classified as a WNT tumor (positive for CTNNB1 and DKK1). 29/55 were SHH tumors (positive for GLI and SFRP1 staining). 16/55 were group 4 tumors (positive for KCNA1) and 9/55 were group 3 tumors (positive for NPR3). Immunohistochemical analysis of human cerebellar development was performed on FFPE specimens obtained from UHN autopsy archival materials. Murine cerebellar development was also assayed in FFPE. All human and murine samples were obtained and accessed in accordance with institutional research ethics guidelines.

Immunohistochemistry protocol

Antibody to total SMAD-3, purchased from Abcam (Cambridge, UK) (product number: ab28379), was used to stain paraffin-embedded samples of developing murine and human cerebella as well as TMAs of human MBs. 4 μm FFPE sections were de-waxed in five changes of xylene and brought down to water through graded alcohol washes. Heat-induced epitope retrieval was performed using a microwavable pressure cooker. Sections were removed from the hot buffer into warm water and then rinsed in Tris-buffered saline (TBS). Endogenous peroxidases were blocked with 3% hydrogen peroxide. Sections were incubated with primary antibody at 1/500 dilution at room temperature for 1 h. The detection system used was Anti-rabbit ImmPRESS polymer system (Vector Labs, Burlingame, CA, USA). After following kit instructions, color development was performed with freshly prepared NovaRed (Vector labs) or DAB (Vector Labs). Finally, sections were counterstained lightly with Mayer's Haematoxylin, dehydrated in alcohols, cleared in xylene and mounted with Permount mounting medium (Thermo Fisher Scientific, Waltham, MA, USA).

Scanning and evaluation of stained sections

The two TMA slides were scanned and viewed via the Aperio Imagescope program (Aperio, Vista, CA, USA). Quantitative analysis on TMAs was performed using the Aperio Spectrum program. Using this program, an algorithm, able to identify nuclei and quantitate the intensity of staining within this organelle, was designed based on a four-tiered scale, with 0 indicating no staining; 1, weak staining; 2, intermediate staining; and 3, strong staining. TMAs were segmented and annotated to remove any areas or cores that were not amenable to analysis (eg, tumor tissue was absent, tissue was poorly preserved, inadequate amounts of tissue were present) and then analyzed using this algorithm.

Statistical analysis of TMAs

Survival analysis of the TMA data was performed using the GraphPad Prism 5 program (GraphPad Software Inc., La Jolla, CA, USA). Chi-squared tests were used to determine statistical significance of the distribution of "positive" and "negative" samples for given qualitative parameters (ie, primary, recurrent or metastatic disease stage).

RESULTS

Gene expression microarrays identify TGF-β involvement in aggressive MB behavior

We isolated RNA from FFPE samples of both pediatric and adult patients. Many samples including all of the pediatric tumors yielded poor-quality RNA that was unsuitable for microarray analysis. Our human samples, therefore, consisted of eight matched samples from four adult MB patients, which met the highest quantity and quality standards as described above in Materials and Methods (Table 1). These included four primaries, three recurrences and one metastatic tumor. Patient-matched samples were used in the hopes of reducing some of the heterogeneity inherent to an outbred human population. NanoString molecular subtyping of these samples revealed that all eight belong to the sonic hedgehog (SHH) subgroup seen in about 25% of all human MB cases and in the majority of adult MBs (10, 31, 37, 41, 48). Although pediatric and adult MBs differ with regards to many clinicopathological features (32, 41), within the SHH subtype, they are comparable. Pediatric and adult SHH tumors share a similar distribution of histology (comprising the majority of desmoplastic tumors), genetic aberrations (9q and 10q loss), overall and progression free survival, and of course dysregulation of the SHH pathway as the driving force behind tumorigenesis (41). We identified 411 genes whose expression was significantly different between the primary and recurrent/metastatic samples (Figure 1).

The murine samples consisted of RNA extracted from fresh frozen tumor tissue derived from the Ptch and Smo/Smo mouse models of MB. Ptch mice are hemizygous for the normal patched-1 gene, which is the inhibitory receptor of the SHH pathway, crucial in cell and organ development, including the cerebellum (14, 21, 22, 43). These mice recapitulate the SHH molecular subtype of MB. They form well-circumscribed tumors, which rarely invade adjacent tissue and almost never metastasize (23). Smo/Smo mice carry an activating mutation in both copies of the smoothened gene, which is the activating receptor in the SHH pathway, normally inhibited by patched when unbound to ligand (23). This mouse model allows for constitutive activation of the

Table 1. Clinical characteristic of human microarray cohort.

Sex no.	
Male	2
Female	2
Patient age at primary disease, years	
Median	27
Range	19–36
Patient age at Rec/Met disease, years	
Median	33
Range	25–44
Recurrence no.	3
Metastasis no.	1
Location of metastasis	Spinal cord
Time to first relapse event, months	
Median	54.5
Range	43–72
Overall survival, %	
Alive	0
Dead	100
Molecular subtype of primary tumors, %	
WNT	0
SHH	100
Group 3	0
Group 4	0
Molecular subtype of Met/Rec tumors, %	
WNT	0
SHH	100
Group 3	0
Group 4	0
Age of FFPE sample, years	
Median	30.5
Range	15–42

smoothened receptor, regardless of patched receptor status (23). Although this construct also models the SHH subtype of the human disease, these mice exhibit a much more aggressive form of MB. They spontaneously develop tumors at a younger age and at a much higher frequency (23). In addition, approximately 25% of Smo/Smo mice develop leptomeningeal metastasis (23). It is important to note however that the metastatic status of the Smo/Smo tumors used in this study was not known. In this experiment, we identified 386 genes with significantly different expression levels between the two mouse models (Figure 2).

Rather than selecting several candidate genes from our lists for study, a systems-wide approach was taken to uncover the overall molecular events that might be responsible for the gene expression differences, and potentially tumor progression/aggressive behavior (51). This was performed using the IPA program, for both the human and murine datasets. IPA can construct networks using the user's gene list and other candidates that might not be represented on the significant gene list, based on the program's knowledge base (51). It generates sets of networks with a maximum number of genes or proteins per network of 35 (51). A score of significance is assigned to each network, with a score of 2 signifying a 1 in 100 chance that the genes in the network are clustered together based on random chance (51).

Using this software, we were able to identify TGF-β as a node of significance in datasets from both species (Figure 3). The significance score for this network was 34 and 39 in the human and murine sets, respectively. There were no gene orthologs that were present in both the human and murine datasets. Furthermore, TGF-β was one of the few common nodal genes present in a given network in both species.

Smad3 nuclear positivity is a prognosticator of good overall survival in MB

To characterize the activity of the TGF-β pathway in MB, we analyzed two tissue microarrays (TMAs), composed of different subtypes and stages of the human disease. Immunohistochemical staining of TGF-β ligands is ineffective as this technique is not suitable for diffusible molecules. In addition, the presence or absence of cell surface receptors is not an ideal indicator of pathway activation at specific points during disease progression (39, 47, 49). To find an appropriate surrogate for TGF-β pathway status that could be assessed by immunohistochemical means, we looked to downstream signaling mediators of this pathway.

TGF-β signaling is quite complex and characterized by two streams of signal transduction: the canonical pathway, mediated by

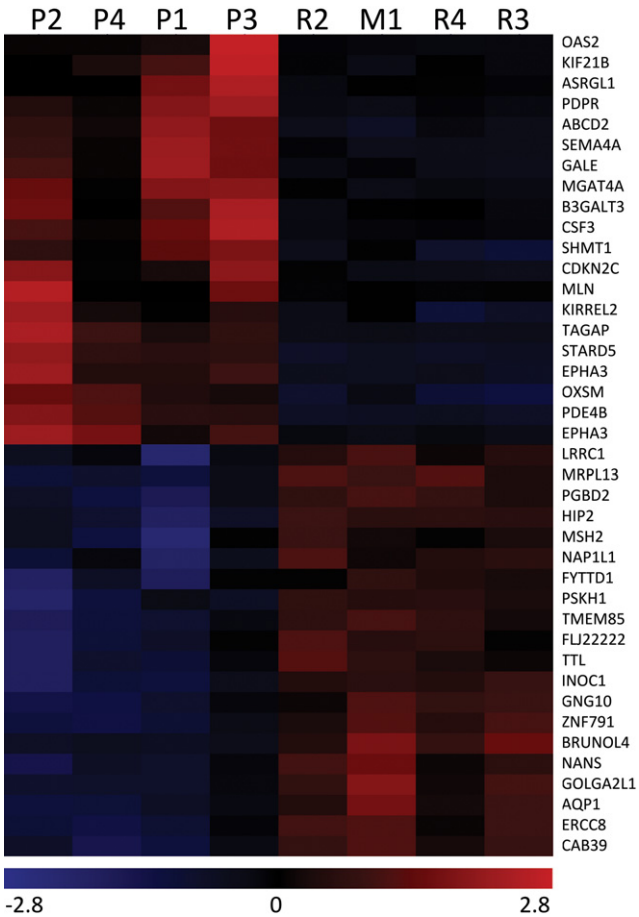

Figure 1. Heat map of human data representing top 20 significant genes with an absolute fold change of 1.5 or greater. P1-P4 = primary samples; R1-R3 = recurrent samples, M1 = metastatic sample.

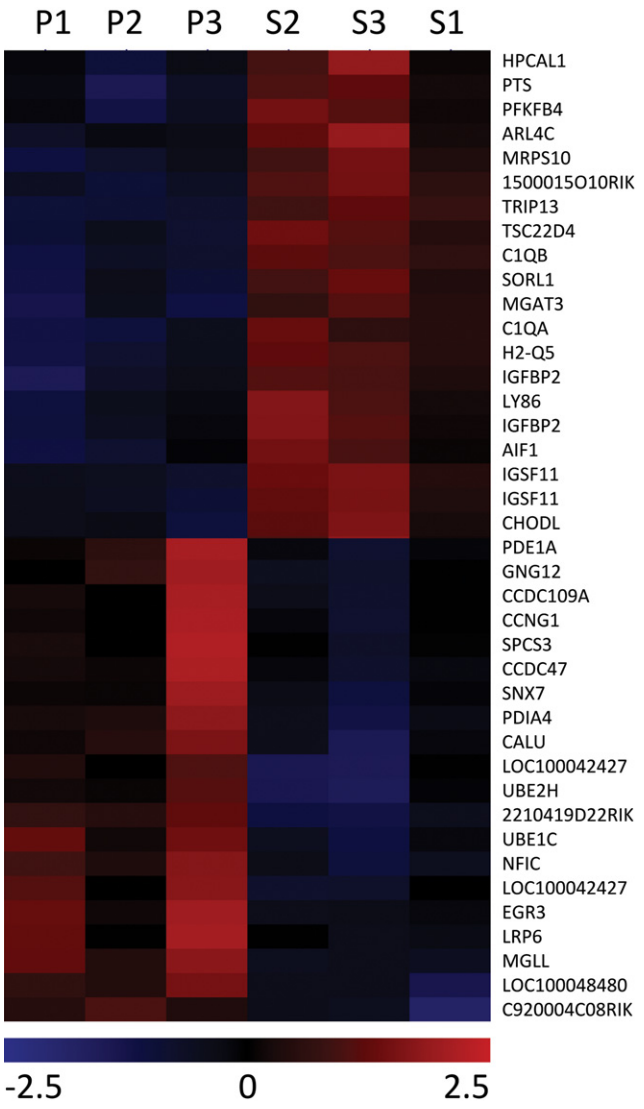

Figure 2. Heat map of murine data representing top 20 significant genes with an absolute fold change of 1.5 or greater. P1-P3 = patch tumors; S1-S3 = Smo/Smo tumors.

Smad2 and 3 proteins, and the non-canonical pathway, which can act through a variety of promiscuous intracellular messengers, including MAPK, PI3K, Rho family of GTPases and mTOR (25, 39, 47, 49). In the canonical pathway, following ligand binding to cell surface TGF-β receptors, the receptor Smads 2 and 3 are recruited and phosphorylated, leading to the formation of a Smad2,3,4 complex, which translocates to the nucleus and acts as a transcription factor to modulate gene expression and cellular behavior (39, 47, 49). Although it has been shown that the Smad proteins are not exclusively part of the TGF-β pathway and can sometimes act promiscuously, they are a much more specific marker of TGF-β signaling than mediators of non-canonical signaling (25, 39, 45, 46). Therefore, we chose the nuclear localization of Smad3 as a surrogate marker for TGF-β activation in tissues.

TMAs were scored both qualitatively and quantitatively and designated as either "negative" or "positive" for nuclear Smad3. Qualitatively, a range of staining intensities was observed. In cases of absent, weak or cytoplasmic staining, the sample was designated as "negative"; "positive" tumors showed intermediate or strong levels of staining. For quantitation, a cutoff of ≥40% average nuclear positivity was used to define positive samples.

The first TMA consisted of primary MB samples. Survival analysis for all patients, by qualitative and quantitative methods, showed a clear and significant difference in overall survival (OS) between positive- and negative-stained tumors (Figures 4A and B). Positivity for nuclear Smad3 staining provided a survival advantage to patients. When looking at specific subgroups of patients, nuclear Smad3 negativity also indicated poor OS. Dividing patients on the basis of histology, the same trend was observed, which was statistically significant within classical tumors, but not in the desmoplastic and large cell anaplastic categories (Figures 4C–E). However, these latter subgroups displayed a much smaller total number of patients. Different molecular subgroups also displayed a similar trend (Figures 4F–H). There was only one WNT tumor represented on the TMA; therefore, this subgroup could not be analyzed. The survival difference between positively and negatively stained tumors was statistically significant in the SHH subgroup, which was overrepresented in the TMA, but did not reach statistical significance in the small number of groups 3 or 4 tumors available for analysis. Hence, absence of nuclear Smad3 indicated poor OS, and this trend was consistent across tumor histology and molecular subtypes. That this trend did not reach statistical significance in some of the categories analyzed might be caused by low sample numbers within subcategories.

The second TMA consisted of MBs at varying stages of the disease, including primary, recurrent and metastatic tumors. Thirty-eight primary, 16 recurrent and five metastatic tumors were amenable to scoring (ie, enough preserved tissue was present in the core). Comparing primary and recurrent tumors, no significant difference was found between the frequency of positive- and negative-stained samples (Figure 5A). However, in regards to metastatic tumors, 100% of these (5/5) were negative for nuclear Smad3. This bias toward negative Smad3 staining within the metastatic tumors was statistically significant using a Chi-squared test despite the low number of overall samples (Figure 5A).

To see whether Smad3 nuclear staining might predict recurrence or metastasis at early stages of the disease, we compared staining of primary tumors that had recurred or metastasized to those that had not. No significant difference in the distribution of positive- or negative-stained tumors was observed (Figure 5B). Therefore, although nuclear Smad3 staining was significantly correlated with metastasis, it was not predictive of metastasis or recurrence.

mRNA levels of Smad3 in primary MB samples do not correlate with survival

To evaluate whether similar trends in survival and molecular subtype extend to the RNA expression levels of Smad3, we turned to two large mRNA expression databases derived from primary MBs. In both cohorts, Smad3 mRNA was significantly increased in the WNT and depressed in group 4 tumors (Figure 6A). It is interesting to note the difference in overall survival between these two subtypes of MB. WNT tumors have a very favorable outcome, with averages of 90% progression free and overall survival rates (5, 10, 30, 31, 36, 48). Group 4 tumors display significantly worse

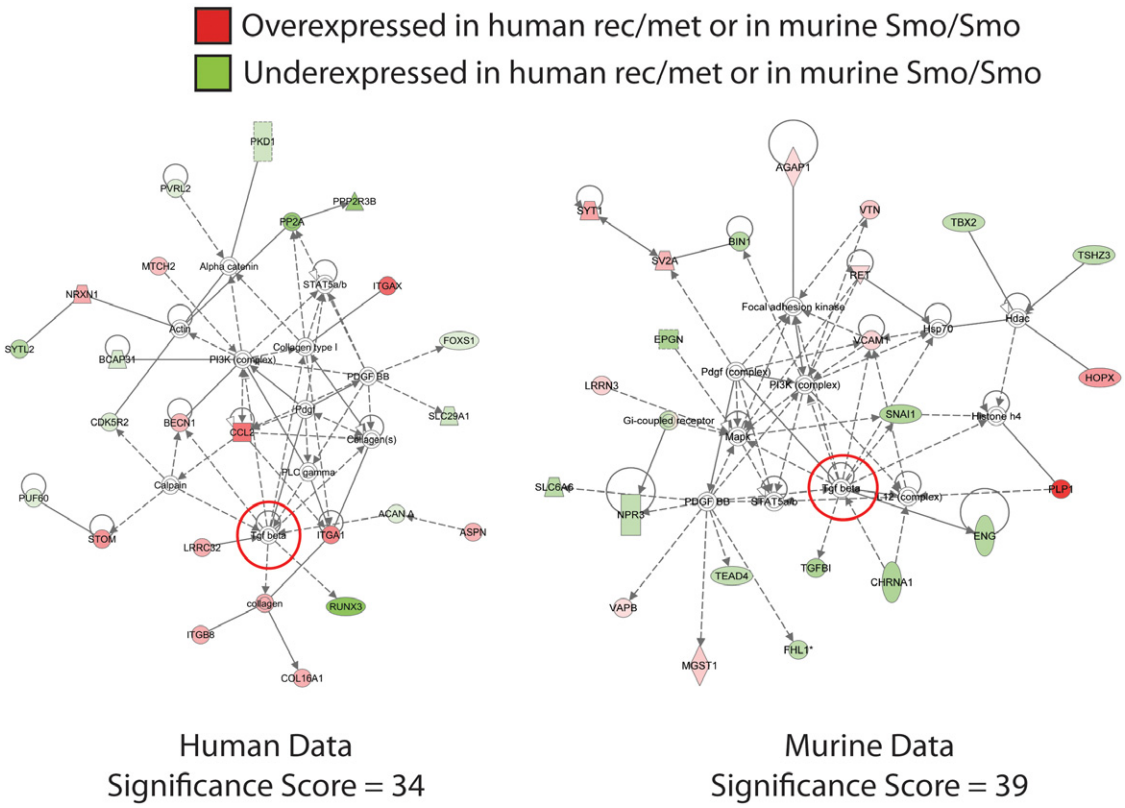

Figure 3. Ingenuity Pathway Analysis revealed TGF-β as a node, linking a subset of the genes within the microarray identified list, in a statistically enriched network in both the human and murine species.

progression free and overall survival when compared to the WNT subgroup (5, 10, 30, 31, 36, 48). In relation to the four major molecular subtypes of MB, group 4 tumors can be classified as having intermediate progression and survival rates, comparable to SHH but better than group 3 tumors (5, 10, 30, 31, 36, 48).

In spite of the difference in Smad3 mRNA expression levels among MB molecular subgroup, no difference in patient survival between high and low Smad3 expressers was observed (Figure 6B). mRNA levels are not always directly correlated with protein amount or concentration. Smad3 mRNA and protein kinetics might, therefore, be unassociated and distinct, accounting for the different results between our TMA and mRNA expression survival analyses. Conversely, the lack of any survival advantage in the high-Smad3 mRNA expressers might suggest that Smad3 mRNA or protein levels, alone, are not prognosticators of outcome in MB; rather, the activation of the canonical arm of the TGF-β pathway (indicated by nuclear localization of Smad3) is responsible. As canonical TGF-β pathway activation is only partially dependant on Smad3 mRNA and protein levels, significant survival differences are not observed using this parameter.

Smad3 immunohistochemistry defines putative tumor precursor cells in cerebellar development

MB is considered an embryonal tumor and thought to arise through transformation of primitive cells during cerebellar development (14, 16, 22, 43). As a parallel to our immunohistochemical investigation of human MBs, we elected to take a similar approach and use immunohistochemistry with anti-Smad3 to detect normal cells in development, which might be precursors to MB.

Cerebellar development in the mouse occurs largely postnatally from day 1 to day 20 postpartum (21, 22, 43). During the early stages of development, from postnatal day 1 to 7 (P1–P7), the granule neuron precursor cells in the external granule layer (EGL) undergo massive rounds of proliferation (14, 21, 22, 43). From P7 to P13, the proliferation rate slowly decreases, as the cells of the EGL begin to mature and migrate through the molecular layer (ML) and into the internal granule layer (IGL) (21, 22, 43). By P20, the macrostructures of the cerebellum are fully developed and the organ closely resembles that of the adult mouse (21).

We stained the murine cerebellum at each of the important developmental milestones, specifically at P1, P7, P13, P20 and 6 weeks of age, for Smad3 and other cellular markers. The EGL was largely negative for nuclear NeuN, a marker of more mature neurons, while staining for nestin, a marker of primitive, undifferentiated cells, was observed throughout the time points examined, as expected. Interestingly, no Smad3 nuclear staining was observed at any time during cerebellar development in this structure (Figure 7A). This result implies that the most immature granule neuron precursors are likely not responsive to or stimulated by TGF-β signaling to induce the canonical arm of the pathway during the lifetime of the EGL.

The greatest number of Smad3-positive cells was observed at the upper border of the emergent IGL and throughout the ML, during early and mid-cerebellar development (Figure 7A). The staining was most intense at P7–P13, when granule neuron precursors of the EGL are differentiating and migrating into the IGL. Smad3 staining patterns were paralleled most closely by NeuN and not by GFAP staining, a marker for astrocytes. This indicates that the majority of Smad3 nuclear positive cells throughout cerebellar development are comprised of maturing cells of neuronal lineage.

At P20 and 6 weeks of age, all compartments of the fully developed cerebellum are negative for nuclear Smad3 staining except for scattered cells adjacent to the Purkinje neurons (Figure 7A). These nuclear Smad3-positive cells seem to also represent a subset of mature neurons as they co-stain for NeuN (Figure 7A).

The development of the human cerebellum is more complex and takes place both *in utero* and postnatally; however, it shares the same basic features and key developmental milestones as the mouse (21, 22, 43). In terms of nuclear Smad3 staining, in humans, the developmental pattern closely mirrors that of the mouse. During early cerebellar development, at embryonic week 26, corresponding to P1 in the mouse (21, 22, 43), most of the EGL and IGL are negative for nuclear Smad3 staining (Figure 7B). At the end of gestation (37–40 weeks), which corresponds to P7–P13 during murine development (21, 22, 43), when cells of the EGL begin to mature and migrate downwards into the IGL, Smad3-positive cells are observed scattered throughout the molecular layer (Figure 7B). At 1 year postpartum, the human cerebellum is almost fully developed (akin to P20 in the mouse) (21, 22, 43) and little nuclear Smad3 staining is observed except, again, in cells adjacent to Purkinje neurons at the border of the molecular and granule cell layers (Figure 7B).

As in the mouse, Smad3 nuclear staining is mirrored most closely by NeuN staining, while little overlap is observed with staining for GFAP (Figure 7B). Therefore, Smad3 nuclear positive

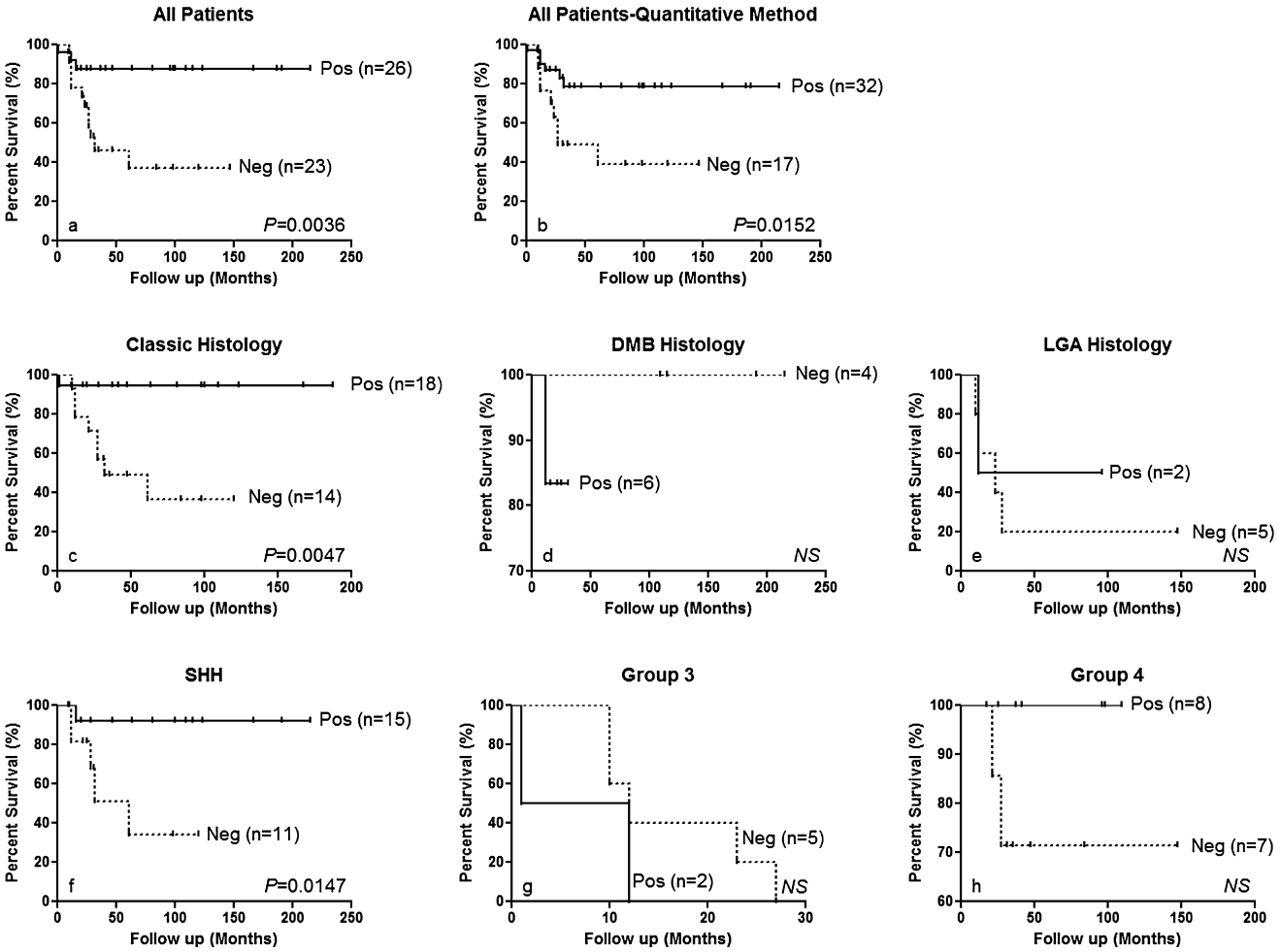

Figure 4. Nuclear Smad3 positivity identifies patients with good overall survival across various patient subclasses. **A.** Evaluation of entire TMA manually and **B.** by quantitative means (spectrum) reveals that nuclear Smad3 positivity is a prognosticator of favorable outcome. **C–E.** patients classified based on tumor histology. **F–H.** patients divided based on molecular subtype. OS = overall survival; DMB = desmoplastic; LGA, = large cell anaplastic; SHH = sonic hedgehog.

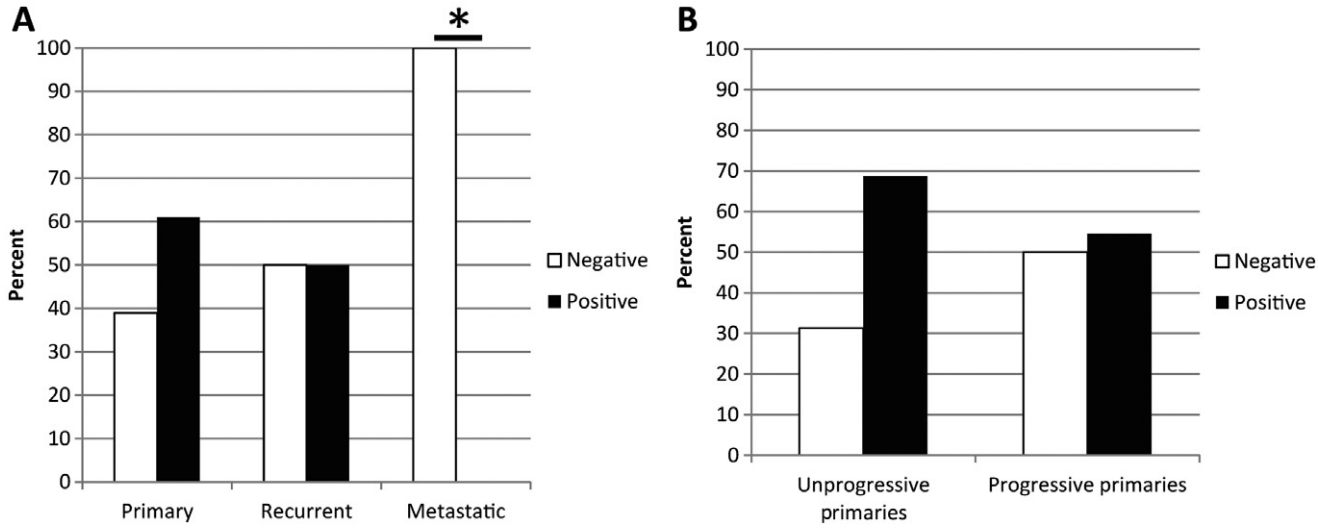

Figure 5. TMA comprised of patients with MBs at different stages of disease progression. **A.** Metastatic tumors stain negatively for nuclear Smad3 ($P = 0.0186$); n (primary) = 38, n (recurrent) = 16, n (metastatic) = 5. **B.** There is no difference between the frequencies of positive and negative staining for nuclear Smad3 in primary tumors that recur/metastasize ($n = 22$) and those that do not ($n = 16$).

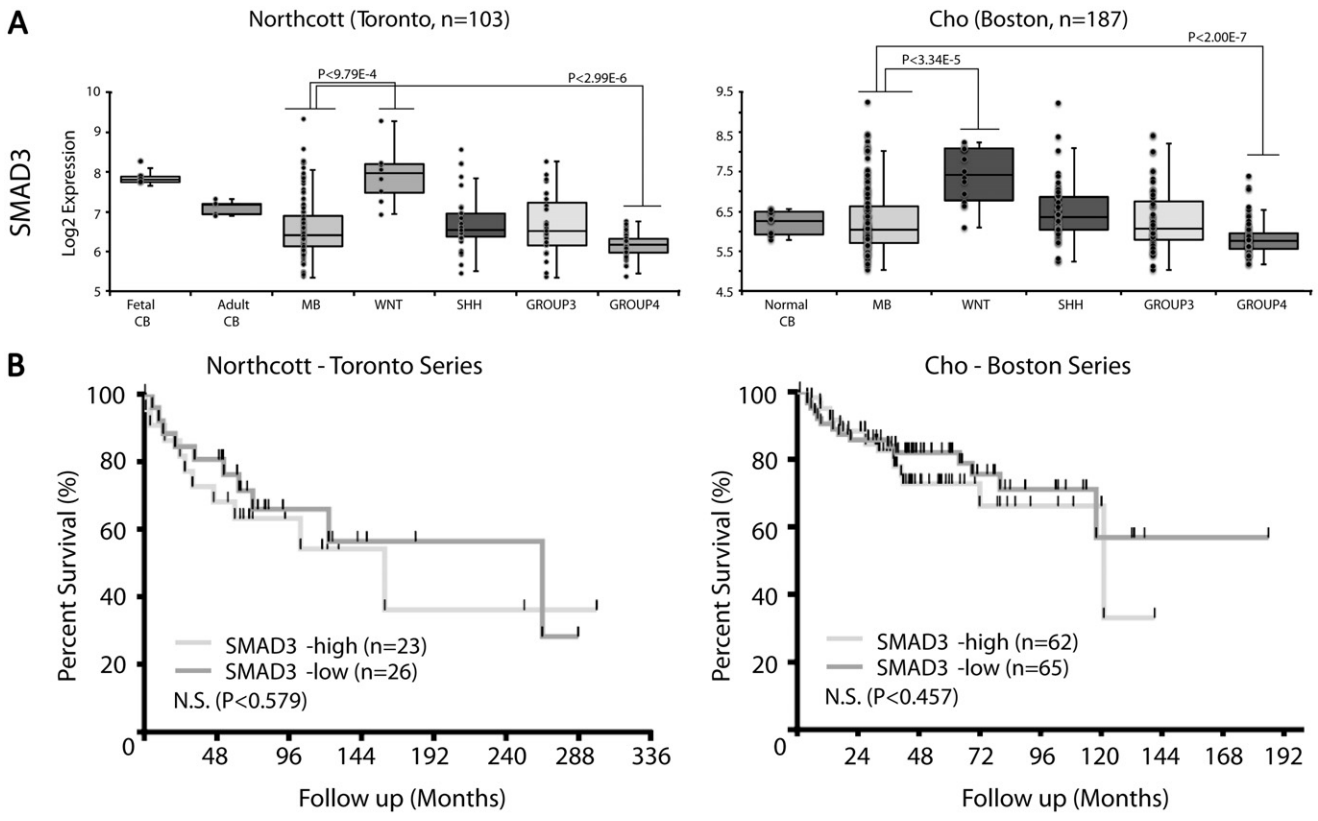

Figure 6. mRNA levels of Smad3 in primary MB tumors. **A.** Smad3 mRNA is significantly upregulated in WNT and depressed in group 4 subtypes in two large gene expression databases of primary MB. **B.** No survival difference is observed between high vs. low Smad3 expressers.

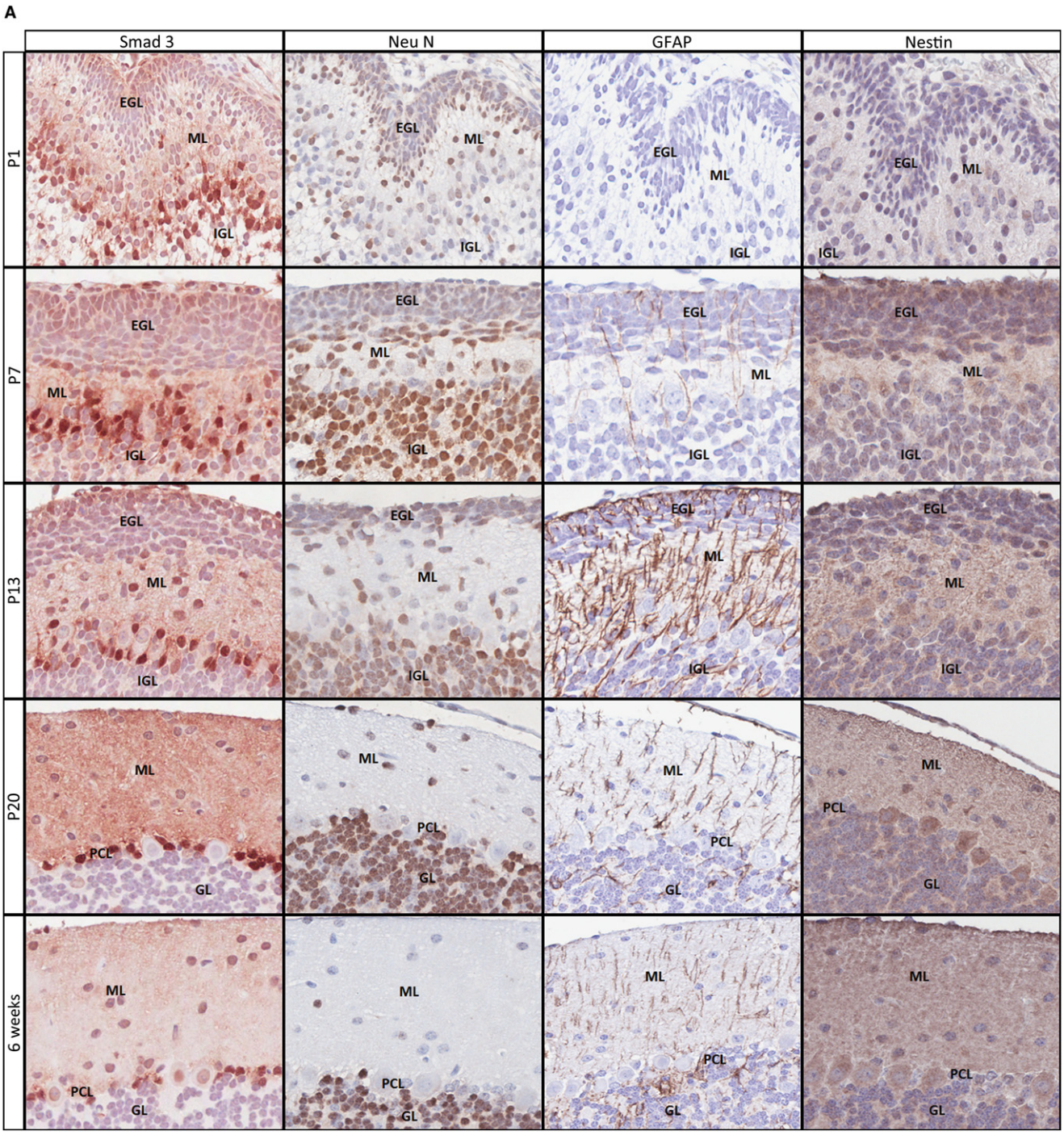

Figure 7. Smad3 nuclear localization during (**A**) human (20× mag) and (**B**) murine (40× mag) cerebellar development. The greatest staining is observed during the beginning of granule neuron precursor (GCP) maturation and migration out of the EGL (P7-13 in the mouse, 26–40 weeks gestation in the human). Almost no staining for this marker is observed in the developing EGL or in the mature granule neuron layer. The Smad3 staining pattern is closely paralleled by NeuN, a marker of mature neurons but not by a marker of astrocytes (GFAP) or primitive neuronal cells (nestin). In the mature cerebellum, nuclear Smad3 staining is largely absent except in a subset of cells adjacent to Purkinje neurons. These cells stain for NeuN but not for GFAP or nestin, indicating they are of neuronal lineage. EGL = external granule layer; ML = molecular layer; IGL = internal granule layer; GL = granule layer; PCL = Purkinje cell layer; GFAP = glial fibrillary acidic protein.

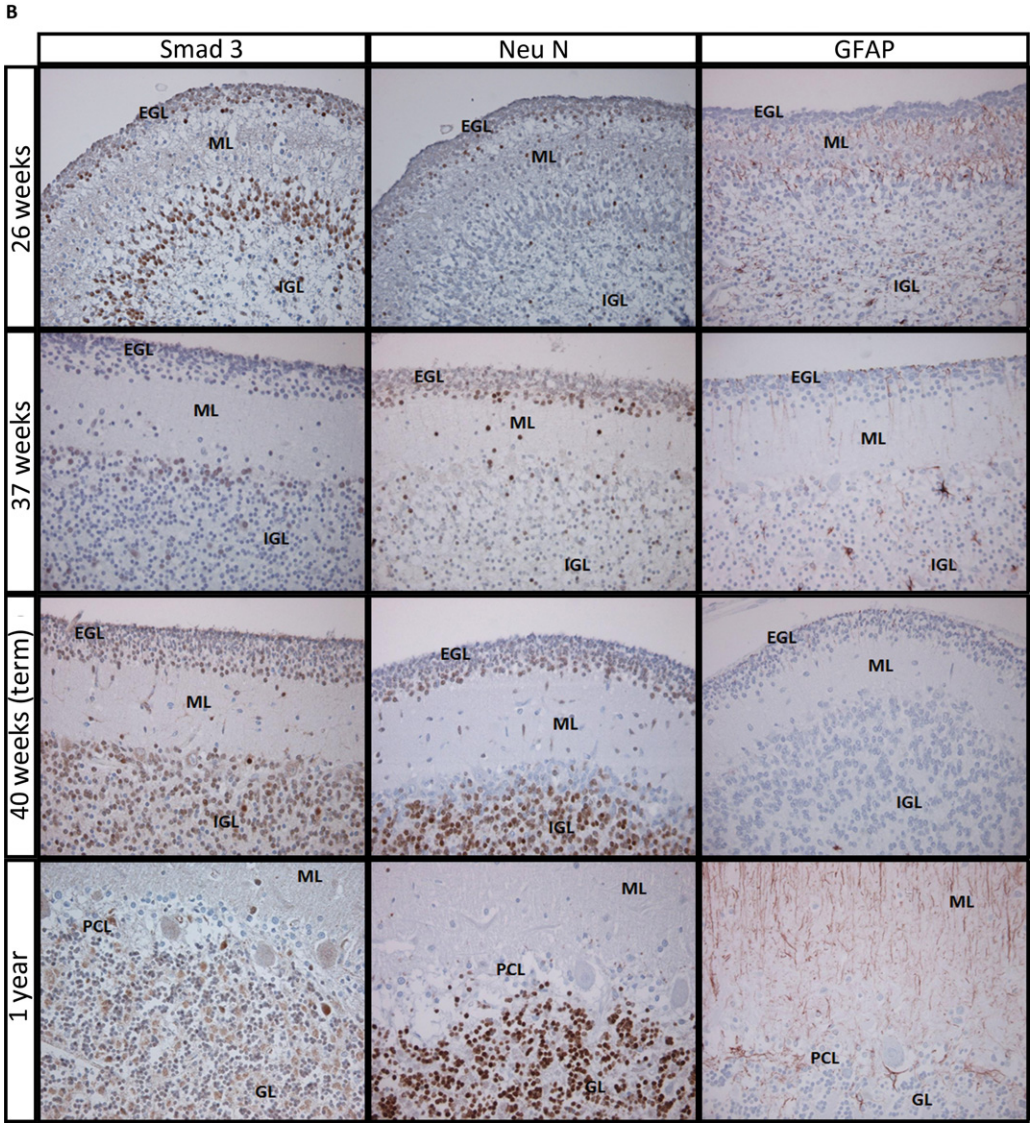

Figure 7. *Continued*

cells in humans also represent a subset of more mature neuronal cells during development.

Hence, in both species, Smad3 nuclear positivity is a transient event, observed during the maturation, differentiation and migration of primitive neuronal precursors. In this way, Smad3 marks a population of more mature granule neuron precursors probably during their migration out of the EGL, to their final destination in the IGL. It is quite possible that these are the cell of origin of the SMAD3-positive good prognosis MBs.

CDK5: a potential mediator of TGF-β activity in MB

In normal cells, cessation of proliferation is a key prerequisite for differentiation and migration (6, 35, 38, 42, 54). One of the major cellular effects of TGF-β canonical signaling is the induction of cytostasis via the transcriptional activation of cyclin-dependant kinase (CDK) inhibitors (CKI) (42). We mined our array gene profiling data for the expression of these proteins to determine whether they play a role in TGF-β pathway regulation in MB. We identified one gene, CDKN2C (p18), an inhibitor of CDK4 and CDK6 (15), downregulated (1.65-fold) in our human list. No CKI proteins were identified in the murine data.

We also identified several proteins associated with the atypical, neuronal CDK (6, 35, 38, 50, 54), CDK5 in both species. CDK5R2 and CDK5RAP2 were both downregulated, 2.1- and 2.7-fold respectively, within metastatic human tumors, whereas CDK5RAP3 was upregulated 1.7-fold in the Smo transgenic mice. CDK5 has been shown to be important for the induction of cell cycle arrest, differentiation and migration of neuronal cells both *in vitro* and *in vivo* (6, 35, 38, 50, 54). Specifically, the expression of

this protein is high in postmitotic cells and its loss leads to reentry into the cell cycle (6, 54). In addition, knockout of CDK5 within the nervous system leads to significant abnormalities in the developmental program of neurons, including granule neuron precursors, as evidenced by the presence of immature, proliferating cells within compartments that are normally populated by mature postmitotic neurons and perinatal mortality (38, 54). Finally, it has also been demonstrated that, at least in primary sensory neurons, TGF-β1 regulates CDK5 activity (50).

In the context of MB, it remains to be determined whether functional crosstalk exists between the CDK5 and TGF-β pathways. However, given the elucidated cellular effects of CDK5 and our observations regarding TGF-β in MB, these molecules remains an attractive avenue for investigation in order to link the cell cycle, differentiation and migration defects that underlie cancer and metastasis.

DISCUSSION

Over the past decades, advances made in the understanding of MB have led to a great increase in the overall survival rate, as high as 75%, for patients suffering from this tumor (3, 11, 21, 43). A combination of surgery, craniospinal radiation and chemotherapy is largely responsible for this success (21, 43). Aggressive treatment has also spelled serious neuroendocrine side effects and a steep decline in quality of life for patients post-therapy (21, 43). A major factor that compounds the problem is that current clinical stratification criteria do not effectively identify "low-/standard-risk" patients with resistant disease or "high-risk" patients who might be over treated (3, 21, 43).

To date, much of the research on MB has focused on the process of tumorigenesis and growth (53). As such, the molecular mediators of metastasis and progression remain poorly characterized (53). To further identify pathways of signaling that contribute to aggressive MB behavior, we performed an unbiased, whole genome expression study of primary and recurrent/metastatic human tumors as well as indolent and aggressive murine MBs. We employed a novel strategy by integrating data from a small set of samples of different source RNA quality (FFPE vs. fresh frozen tumors) and from two different species (human and mouse). We also used a systems-wide approach in the analysis of our data, in order to identify important and conserved pathway perturbations present in both species.

We identified the TGF-β as a potential contributor to the pathogenic behavior of MB. Furthermore, we showed that nuclear Smad3 positivity, a major downstream component of the canonical TGF-β pathway, was a prognosticator of good overall survival across many subcategories of patients, including tumor histology and molecular subtype, whereas negative Smad3 nuclear staining correlated with metastatic MB but showed no association or predictive value for recurrence or metastasis of the disease.

All samples that were transcriptionally profiled consisted of adult MB patients. The TMAs used for validating the role of TGF-β at different stages of MB disease progression consisted primarily of adult patients. However, the samples used in the determination of the link between TGF-β pathway activation and patient outcome consisted mostly of pediatric tumors. Future studies are necessary to determine the exact role of the TGF-β pathway in pediatric vs. adult patients and the extent of similarity in the function of this signaling axis in MB of patients with various age demographics.

The survival advantage observed for the Smad3 nuclear positive subset was not as a result of segregation of WNT tumors, known to have excellent prognosis, from the other molecular subtypes as only one WNT tumor was present on our TMA. Hence, although Smad3 and indeed the TGF-β signaling have been shown to be highly cooperative with the WNT pathway, the survival advantage observed for Smad3 nuclear positive tumors cannot be solely attributed to WNT activation, a known marker of good prognosis in MB.

In addition, group 3, group 4 and WNT tumors were poorly represented, while our TMA was enriched for SHH tumors. One possibility that might account for the fact that nuclear Smad3 positivity was not correlated with survival in WNT, group 3 and group 4 tumors is the low numbers of these samples that precluded statistical analysis. An alternative explanation, especially in the case of group 3 and group 4 tumors, might be differential response to TGF-β caused by karyotypic divergence (26). Using a variety of embryonal tumor, including two MB cell lines, it has been previously shown that the number of genetic changes is important in determining the type of response to TGF-β stimulation (26). Tumors with highly unstable genomes are stimulated to proliferate in the presence of TGF-β, whereas this molecule retains its cytostatic abilities in genetically quite tumor environments (26). This same observation has been made in the context of gliomas (26).

MycC, amplified in group 3, and Otx2, amplified in both groups 3 and 4 tumors play important roles in cell and organismal survival and are known factors for poor prognosis in MB (10, 31, 48). Previous reports have shown that, in part, the cytostatic/pro-apoptotic effects of canonical TGF-β and BMP signaling are dependent on inhibition of oncogenic c-Myc activity (24). Conversely, reports that indicate the requirement of c-Myc in oncogenic TGF-β signaling (eg, induction of epithelial-to-mesenchymal transition; EMT) also exist (3). In neuroblastoma cells, n-Myc has been shown to regulate the expression of a microRNA (miR-335) that modulates TGF-β noncanonical signaling (34). Otx2 is a transcription factor critical for brain patterning and development whose expression in the neuroectoderm is regulated by Smad-dependent TGF-β signaling (27). Genetic defects in the Myc family proteins and Otx2 might be important in counteracting the cytostatic and tumor suppressive effects and perhaps potentiating oncogenic TGF-β activity within more aggressive subtypes. Therefore, Smad3 loss within the group 3 and group 4 tumors might be related to the acquisition of these and other, as of yet undetermined, genetic events characteristic of these poor prognosis subtypes. It is possible that TGF-β signaling has different pathophysiological effects within different subtypes of MB. From this study, it is clear that the TGF-β pathway is important in SHH-driven tumors. Further investigation is required to elucidate the exact role and effect of TGF-β within these tumor types.

The survival advantage observed when evaluating Smad3 cellular localization was not recapitulated when looking at Smad3 mRNA levels alone, indicating a role for the canonical arm of the TGF-β pathway rather than Smad3 activity on its own. Potentially, Smad3 mRNA and protein kinetics can be distinct as mRNA levels

are not always directly correlated with protein amount or concentration. Conversely, the lack of any survival advantage in the high Smad3 mRNA expressers might be indicative of a role for the canonical arm of the TGF-β pathway, of which nuclear Smad3 localization is a marker. Hence, Smad3 mRNA or protein levels, alone, would not be prognosticators of outcome in MB as canonical TGF-β pathway activation is only partially dependant on Smad3 mRNA or protein levels.

We also showed that Smad3 expression during development identified a subset of cerebellar neuronal precursors as putative cells of origin for the Smad3-positive MBs. In addition, there seemed to be a developmental role for the TGF-β pathway within the cerebellum. Immunohistochemical staining of developing human and murine cerebella, revealed a similar pattern of Smad3 nuclear localization in both species. Staining spatiotemporally coincided with the maturation and migration of granule neuron precursors (GCP) out of the EGL and into the developing IGL. Almost no staining for this marker was observed in the developing EGL or in the mature granule neuron layer. Therefore, Smad3 nuclear positivity in the developing cerebellum represented a transient event, observed during the maturation, differentiation and migration of primitive neuronal precursors.

The above observations from MB tumors and cerebellar development are consistent with a putative role for the TGF-β pathway in cell cycle exit, differentiation and migration of cells of neuronal lineage in the cerebellum. A potential downstream mediator of TGF-β that links these cellular processes is CDK5 as associated proteins were dysregulated within both human and murine species examined. CDK5 is an atypical cyclin-dependant kinase that is highly expressed in postmitotic cells of the nervous system (6, 35, 38, 50, 54). In addition, in primary sensory neurons, TGF-β1 has been shown to increase CDK5 and CDK5R1 protein levels with a concomitant increase to CDK5 activity (50). Further investigations are required to demonstrate cooperation between the TGF-β pathway and CDK5 activity in MB, and elucidate their pathobiological role, if any, in this tumor.

The identification of the TGF-β pathway was surprising as this signaling axis has not been widely linked to MB pathogenesis or cerebellar development. Nevertheless, several lines of evidence suggest a role for TGF-β involvement during these processes. In terms of cerebellar development, TGF-β2, the major isoform of TGF-β expressed in the cerebellum is secreted by maturing granule neurons, the suspected cells of origin for at least some subtypes of MB, from postnatal day 3 to about day 13 in the mouse (7). Several studies have shown that this molecule may induce apoptosis, proliferation or maturation of both mature and precursor granule neurons, depending on the environment (9, 12, 28, 29). The time period during which TGF-β2 is expressed coincides with the migration of maturing granule neurons from the EGL of the developing cerebellum to the IGL (21, 22, 43). Cerebellar Purkinje neurons produce and secrete this molecule throughout the lifespan of the mouse (7). It is not surprising, then, that we observe a subset of neuronal cells adjacent to them that stain for nuclear Smad3 in the adult organism. Furthermore, TGF-β1 is constitutively produced by a small but distinct population of cells in the meninges, the most common site for MB metastasis (7). Most recently, it has been shown that CNS-specific knockdown of Smad2, but not Smad3, causes severe cerebellar dysfunction, including delayed maturation and migration of granule neuron precursors (52). In addition, several BMPs, which are part of the same family of proteins, have been implicated in inducing migration and differentiation at several points during cerebellar development including promoting the differentiation and maturation of granule neuron precursors (22, 43).

As with cerebellar development, some evidence exists, suggesting the involvement of the TGF-β pathway in MB. For example, overexpression of FOXG1, a repressor of TGF-β-induced cytostasis, seems to be a common, early event in MB (1). When looking at the large gene profiling studies of primary MBs that uncovered the molecular subtype paradigm for this tumor, components of this pathway seem to be dysregulated in many subtypes of the disease (WNT: Smad3, TGFBI; SHH: TGFB2; group 3: TGFBR3, TGFB1) (5, 30, 36). In addition, various molecules associated with the TGF-β pathway have been linked to MB pathogenesis. miR-21 has recently been shown to be involved in MB metastasis (19). This microRNA has also been linked to the TGF-β pathway in other contexts and thought to regulate and be regulated by this signaling axis (19). The bone morphogenic proteins (BMPs), which are part of the TGF-β superfamily, have also been implicated in MB pathogenesis (2, 13, 14, 20, 22, 43, 55).

In this study, we clearly link TGF-β to SHH-driven MB pathogenesis. We show that nuclear Smad3 staining is a prognosticator of favorable outcome in classic tumor histology and SHH molecular subtypes of the disease. This survival advantage is only observed when looking at protein localization (ie, nuclear localization of Smad3) as Smad3 mRNA levels do not replicate these dramatic results. This suggests that canonical TGF-β signaling, of which Smad3 nuclear localization is a marker, is the true prognosticator of patient survival. Recent evidence, from other cancer types, indicates that an imbalance between the canonical and non-canonical arms of TGF-β signaling might be responsible for converting this molecule from a tumor suppressor to a tumor promoter (39). Therefore, as tumor malignancy increases Smad-dependant canonical signaling decreases, accompanied by a concomitant increase in signaling via Smad-independent, non-canonical pathways and onco-stimulatory effects of TGF-β (39).

Data obtained from our developmental staining also gives us avenues for further investigation into the mechanistic role this pathway might play in MB. Although it is possible that Smad3 nuclear localization is simply a marker for good prognosis MB, it is also likely that canonical TGF-β signaling has an active role in MB pathogenesis. As, in the normal developing cerebellum, cells positive for Smad3 nuclear localization exist, and different MB subtypes have different cells of origin (17, 18), it is possible that these are the cells of origin of good prognosis MB. Conversely, during cerebellar development, nuclear Smad3 positivity marks a population of more mature/maturing granule neuron precursors. Nuclear Smad3-positive MBs might demarcate a subset of tumors that are in a less primitive state that is more responsive to environmental and developmental cues. This might be the basis for the observed survival advantage of this group of tumors. Further investigation into the mechanistic role of TGF-β is required to fully elucidate the role of this pathway in MB.

To our knowledge, this is the first time that a clear link between the TGF-β pathway and MB pathogenesis has been made. From this research, it seems that canonical activation of this pathway leads to better prognosis for patients.

REFERENCES

1. Adesina AM, Nguyen Y, Mehta V, Takei H, Stangeby P, Crabtree S *et al* (2007) Foxg1 dysregulation is a frequent event in medulloblastoma. *J Neurooncol* **85**:111–122.
2. Alvarez-Rodriguez R, Barzi M, Berenguer J, Pons S (2007) Bone morphogenic protein 2 opposes SHH-mediated proliferation in cerebellar granule cells through a TIEG-1-based regulation of nMyc. *J Biol Chem* **282**:37170–37180.
3. Amatangelo MD, Goodyear SM, Varma D, Stearns ME (2012) c-Myc expression and MEK1 induced Erk2 nuclear localization are required for TGF-beta induced epithelial-mesenchymal transition and invasion in prostate cancer. *Carcinogenesis* [Epub ahead of print; doi:10.1093/carcin/bgs227].
4. Bourdeaut F, Miquel C, Alapetite C, Roujeau T, Doz F (2011) Medulloblastoma: update on a heterogeneous disease. *Curr Opin Oncol* **23**:630–637.
5. Cho YJ, Tsherniak A, Tamayo P, Santagata S, Ligon A, Greulich H *et al* (2011) Integrative genomic analysis of medulloblastoma identifies a molecular subgroup that drives poor clinical outcome. *J Clin Oncol* **29**:1424–1430.
6. Cicero S, Herrup K (2005) Cyclin-dependant kinase 5 is essential for neuronal cell cycle arrest and differentiation. *J Neurosci* **25**:9658–9668.
7. Constam DB, Schmid P, Aguzzi A, Schachner M, Fontana A (1994) Transient production of TGF-Beta2 by postnatal cerebellar neurons and its effect on neuroblast proliferation. *Eur J Neurosci* **6**:766–778.
8. de Haas T, Hasselt N, Troost D, Caron H, Popovic M, Zadravec-Zaletel L *et al* (2008) Molecular risk stratification of medulloblastoma patients based on immunohistochemical analysis of Myc, LDHB, and CCNB1 expression. *Clin Cancer Res* **14**:4154–4160.
9. de Luca A, Weller M, Fontana A (1996) TGF-b induced apoptosis of cerebellar granule neurons is prevented by depolarization. *J Neurosci* **16**:4174–4185.
10. Ellison DW, Dalton J, Kocak M, Nicholson SL, Fraga C, Neale G *et al* (2011) Medulloblastoma: clinicopathological correlates of SHH, WNT, and non-SHH/WNT molecular subgroups. *Acta Neuropathol* **121**:381–396.
11. Ellison DW, Kocak M, Dalton J, Megahed H, Lusher ME, Ryan SL *et al* (2011) Definition of disease-risk stratification groups in childhood medulloblastoma using combined clinical, pathologic, and molecular variables. *J Clin Oncol* **23**:630–637.
12. Elvers M, Pfeiffer J, Kaltschmidt C, Kaltschmidt B (2005) TGF-b2 neutralization inhibits proliferation and activates apoptosis of cerebellar granule cell precursors in the developing cerebellum. *Mech Dev* **122**:587–602.
13. Fiaschetti G, Castelletti D, Zoller S, Schramm A, Schroeder C, Nagaishi M *et al* (2011) Bone morphogenic protein-7 is a MYC target with prosurvival functions in childhood medulloblastoma. *Oncogene* **30**:2823–2835.
14. Fogarty MP, Kessler JD, Wechsler-Reya RJ (2005) Morphing into cancer: the role of developmental signaling pathways in brain tumor formation. *J Neurobiol* **64**:458–475.
15. Gagrica S, Brookes S, Anderton E, Rowe J, Peters G (2012) Contrasting behaviour of the P18INK4C and P16INK4A tumor suppressors in both replicative and oncogene-induced senescence. *Cancer Res* **72**:165–175.
16. Giangaspero F, Eberhart CG, Haapasalo H, Pietsch T, Wiestler OD, Ellison DW (2007) Chapter 8: medulloblastoma. In: *WHO Classification of Tumors of the Central Nervous System*, DN Louis, H Ohgaki, OD Wiestler, WK Cvenee (eds), pp. 132–140. International Agency for Research on Cancer: Lyon.
17. Gibson P, Tong Y, Robinson G, Thomson MC, Currie DS, Eden C *et al* (2010) Subtypes of medulloblastoma have distinct developmental origins. *Nature* **468**:1095–1099.
18. Gilbertson RJ, Ellison DW (2008) The origins of medulloblastoma subtypes. *Annu Rev Pathol* **3**:341–365.
19. Grunder E, D'Ambrosio R, Fiaschetti G, Abela L, Arcaro A, Zuzak T *et al* (2011) MicroRNA-21 suppresses impedes medulloblastoma cell migration. *Eur J Cancer* **47**:2479–2490.
20. Hallahan AR, Pritchard JI, Chandraratna RA, Ellenbogen RG, Geyer JR, Overland RP *et al* (2003) BMP-2 mediates retinoid induced apoptosis in medulloblastoma cells through a paracrine effect. *Nat Med* **9**:1033–1038.
21. Hatten ME (1999) Central nervous system neuronal migration. *Annu Rev Neurosci* **22**:511–539.
22. Hatten ME, Roussel MF (2011) Development and cancer of the cerebellum. *Trends Neurosci* **34**:134–142.
23. Hatton BA, Villavicenicio EH, Tsuchiya KD, Pritchard JI, Ditzler S, Pullar B *et al* (2008) The Smo/Smo model: hedgehog-induced medulloblstoma with 90% incidence and leptomeningeal spread. *Cancer Res* **68**:1768–1776.
24. Holien T, Vatsveen TK, Hella H, Rampa C, Brede G, Groseth LAG *et al* (2012) Bone morphogenic proteins induce apoptosis in multiple myeloma cells by Smad-dependent repression of MYC. *Leukemia* **26**:1073–1080.
25. Jakowlew SB (2006) Transforming growth factor-beta in cancer and metastasis. *Cancer Metastasis Rev* **25**:435–457.
26. Jennings MT, Kaariainen IT, Gold L, Maciunas RJ, Commers PA (1994) TGF-β1 and TGF-β2 are potential growth regulators for medulloblastomas, primitive neuroectodermal tumors, and ependymomas: evidence in support of an autocrine hypothesis. *Hum Pathol* **25**:464–475.
27. Jia S, Wu D, Xing C, Meng A (2009) Smad2/3 activities are required for induction and patterning of the neuroectoderm in zebrafish. *Dev Biol* **333**:273–284.
28. Kaltschimdt B, Kaltschmidt C (2001) DNA array analysis of the developing rat cerebellum: transforming growth factor-b2 inhibits constitutively activated NF-kB in granule neurons. *Mech Dev* **101**:11–19.
29. Kane CJM, Brown GJ, Phelan KD (1996) Transforming growth factor-b2 both stimulates and inhibits neurogenesis of rat cerebellar granule cells in culture. *Brain Res Dev Brain Res* **96**:46–51.
30. Kool M, Koster J, Bunt J, Hasselt NE, Lakeman A, van Sluis P *et al* (2008) Integrated genomics identifies five medulloblastoma subtypes with distinct genetic profiles, pathway signatures and clinicopathological features. *Plos ONE* **3**:e3088.
31. Kool M, Korshunov A, Remke M, Jones DT, Schlanstein M, Northcott PA *et al* (2012) Molecular subgroups of medulloblastoma: an international meta-analysis of transcriptome, genetic aberrations and clinical data of WNT, SHH, Group 3, and Group 4 medulloblastomas. *Acta Neuropathol* **123**:473–484.
32. Korshunov A, Remke M, Werft W, Benner A, Ryzhova M, Witt H *et al* (2010) Adult and pediatric medulloblastomas are genetically distinct and require different algorithms for molecular risk stratification. *J Clin Oncol* **28**:3054–3060.
33. Li C, Wong WH (2001) Model-based analysis of oligonucleotide arrays: expression index computation and outlier detection. *Proc Natl Acad Sci U S A* **98**:31–36.
34. Lynch J, Fay J, Meehan M, Bryan K, Watters KM, Murphy DM, Stallings RL (2012) MiRNA-335 suppresses neuroblastoma cell invasiveness by direct targeting of multiple genes from the non-canonical TGF-β signaling pathway. *Carcinogenesis* **33**:976–985.
35. Misumi S, Kim TS, Jung CG, Masuda T, Urakawa S, Isobe Y *et al* (2008) Enhanced neurogenesis from neural progenitor cells with

G1/S-phase cell cycle arrest is mediated by transforming growth factor-β1. *Eur J Neurosci* **28**:1049–1059.
36. Northcott PA, Korshunov A, Witt H, Hielscher T, Eberhart CG, Mack S *et al* (2011) Medulloblastoma comprises four distinct molecular variants. *J Clin Oncol* **29**:1408–1414.
37. Northcott PA, Shih DJ, Remke M, Cho YJ, Kool M, Hawkins C *et al* (2012) Rapid, reliable and reproducible molecular sub-grouping of clinical medulloblastoma samples. *Acta Neuropathol* **123**:615–626.
38. Ohshima T, Gilmore EC, Longenecker G, Jacobowitz DM, Brady RO, Herrup K, Kulkarni AB (1999) Migration defects of CDK5(-/-) neurons in the developing cerebellum is cell autonomous. *J Neurosci* **19**:6017–6026.
39. Parvani JG, Taylor MA, Schiemann WP (2011) Noncanonical TGF-Beta signaling during mammary tumorigenesis. *J Mammary Gland Biol Neoplasia* **16**:127–146.
40. Pfister SM, Korshunov A, Kool M, Hasselblatt M, Eberhart C, Taylor MD (2010) Molecular diagnostics of CNS embryonal tumors. *Acta Neuropathol* **120**:553–566.
41. Remke M, Hielscher T, Northcott PA, Witt H, Ryzhova M, Wittmann A *et al* (2011) Adult medulloblastoma comprises three major molecular variants. *J Clin Oncol* **29**:2717–2723.
42. Reynisdottir I, Polyak K, Iavarone A, Massagu J (1995) Kip/Cip and Ink4 Cdk inhibitors cooperate to induce cell cycle arrest in response to TGF-β. *Genes Dev* **9**:1831–1845.
43. Roussel MF, Hatten ME (2011) Cerebellum development and medulloblastoma. *Curr Top Dev Biol* **94**:235–292.
44. Saeed AI, Sharov V, White J, Li J, Liang W, Bhagabati N *et al* (2003) TM4: a free, open-source system for microarray data management and analysis. *Biotechniques* **34**:374–378.
45. Saeed AI, Bhagabati NK, Braisted JC, Liang W, Sharov V, Howe EA *et al* (2006) TM4 microarray software suite. *Methods Enzymol* **411**:134–193.
46. Tamayo P, Cho YJ, Tsherniak A, Greulich H, Ambrogio L, Schouten-van Meeteren N *et al* (2011) Predicting relapse in patients with medulloblastoma by integrating evidence from clinical and genomic features. *J Clin Oncol* **29**:1415–1423.
47. Taylor MA, Lee YH, Schiemann WP (2011) Role of TGF-b and the tumor microenvironment during mammary tumorigenesis. *Gene Expr* **15**:117–132.
48. Taylor MD, Northcott PA, Korshunov A, Remke M, Cho YJ, Clifford SC *et al* (2012) Molecular subgroups of medulloblastoma: the current concensus. *Acta Neuropathol* **123**:456–472.
49. Tian M, Schiemann WP (2009) The TGF-beta paradox in human cancer: an update. *Future Oncol* **5**:259–271.
50. Utreras E, Keller J, Terse A, Prochazkova M, Iadarola MJ, Kulkarni AB (2012) Transforming growth factor-β1 regulates CDK5 activity in primary sensory neurons. *J Biol Chem* **287**:16817–16829.
51. Varambally S, Dhanasekaran SM, Zhou M, Barrette TR, Kumar-Sinha C, Sanda MG *et al* (2002) The polycomb group protein EZH2 is involved in progression of prostate cancer. *Nature* **419**:624–629.
52. Wang L, Nomura M, Goto Y, Tanaka K, Sakamoto R, Abe I *et al* (2011) Smad2 protein disruption in the central nervous system leads to aberrant cerebellar development and early postnatal ataxia in mice. *J Biol Chem* **286**:18766–18774.
53. Wu X, Northcott PA, Dubuc A, Dupuy AJ, Shih DJ, Witt H *et al* (2012) Clonal selection drives genetic divergence of metastatic medulloblastoma. *Nature* **482**:529–533.
54. Zhang J, Cicero SA, Wang L, Romito-Digiacomo RR, Yang Y, Herrup K (2008) Nuclear localization of CDK5 is a key determinant in the postmitotic state of neurons. *Proc Natl Acad Sci U S A* **105**:8772–8777.
55. Zhao H, Ayrault O, Zindy F, Kim JH, Roussel MF (2008) Post transcriptional down regulation of ATOH1/MATH1 by Bone Morphogenic Proteins suppresses medulloblastoma development. *Genes Dev* **22**:722–727.